Title

Computational Modeling of Competitive Metabolism between ω3- and ω6-Polyunsaturated Fatty Acids in Inflammatory Macrophages

Journal

The Journal of Physical Chemistry B, 120(33)

ISSN

1520-6106

Authors

Gupta, Shakti
Kihara, Yasuyuki
Maurya, Mano R
et al.

Publication Date

2016-08-25

DOI

10.1021/acs.jpcb.6b02036

Peer reviewed

Published in final edited form as:

J Phys Chem B. 2016 August 25; 120(33): 8346–8353. doi:10.1021/acs.jpcb.6b02036.

Computational Modeling of Competitive Metabolism Between ω3- and ω6 Polyunsaturated Fatty Acids in Inflammatory Macrophages

Shakti Gupta[1,#], **Yasuyuki Kihara**[2,#,§], **Mano R. Maurya**[1], **Paul C. Norris**[2,£], **Edward A. Dennis**[2], and **Shankar Subramaniam**[1,3]

Shakti Gupta: shgupta@ucsd.edu; Yasuyuki Kihara: kihara-yasuyuki@umin.net; Mano R. Maurya: mano@sdsc.edu; Paul C. Norris: pcnorris@partners.org; Edward A. Dennis: edennis@ucsd.edu; Shankar Subramaniam: shankar@ucsd.edu

[1]Department of Bioengineering and San Diego Supercomputer Center, University of California at San Diego, 9500 Gilman Drive, La Jolla, CA 92093-0412, USA

[2]Department of Chemistry and Biochemistry and Pharmacology, School of Medicine, University of California at San Diego, 9500 Gilman Drive, La Jolla, CA 92093-0601, USA

[3]Departments of Computer Science and Engineering and Cellular and Molecular Medicine, University of California at San Diego, 9500 Gilman Drive, La Jolla, CA 92093-0651, USA

Abstract

Arachidonic acid (AA), a representative ω6 polyunsaturated fatty acid (PUFA), is a precursor of 2-series prostaglandins (PGs) that play important roles in inflammation, pain, fever, and related disorders including cardiovascular diseases. Eating fish or supplementation with the ω3 PUFAs such as eicosapentaenoic acid (EPA) and docosahexaenoic acid (DHA) are widely assumed to be beneficial in preventing cardiovascular diseases. A proposed mechanism for a cardio-protective role of ω3 PUFAs assumes competition between AA and ω3 PUFAs for cyclooxygenases (COX), leading to reduced production of 2-series PGs. In this study, we have used a systems biology approach to integrate existing knowledge and novel high-throughput data that facilitates a quantitative understanding of the molecular mechanism of ω3 and ω6 PUFAs metabolism in mammalian cells. We have developed a quantitative computational model of the competitive metabolism of AA and EPA via the COX pathway through a two-step matrix-based approach to estimate the rate constants. This model was developed by using lipidomic datasets that were experimentally obtained from EPA-supplemented ATP-stimulated RAW264.7 macrophages. The resulting model fits the experimental data well for all metabolites and demonstrates that the integrated metabolic and signaling networks and the experimental data are consistent with one another. The robustness of the model was validated through parametric sensitivity and uncertainty

Correspondence to: Edward A. Dennis, edennis@ucsd.edu; Shankar Subramaniam, shankar@ucsd.edu.

[#]These authors contributed equally to this work.

[§]Current Address: Department of Molecular and Cellular Neuroscience, Doris Neuroscience Center, The Scripps Research Institute, La Jolla, CA 92037.

[£]Current Address: Harvard Institutes of Medicine Bldg., 77 Avenue Louis Pasteur (HIM 836), Boston MA, 02115

Author's contribution

EAD, SS conceived and designed the study. SG and MM developed the computational methods, and SG, YK and MM performed the flux analysis and wrote the first draft of the manuscript. PCN and EAD were responsible for the experimental data. SS and EAD supervised the overall study and revised the manuscript. All authors have read and approved the final manuscript.

analysis. We also validated the model by predicting the results from other independent experiments involving AA and DHA supplemented ATP-stimulated RAW264.7 cells, using the parameters estimated with EPA. Furthermore, we showed that the higher affinity of EPA binding to COX compared to AA was able to inhibit AA metabolism effectively. Thus, our model captures the essential features of competitive metabolism of ω3 and ω6 PUFAs.

Graphical abstract

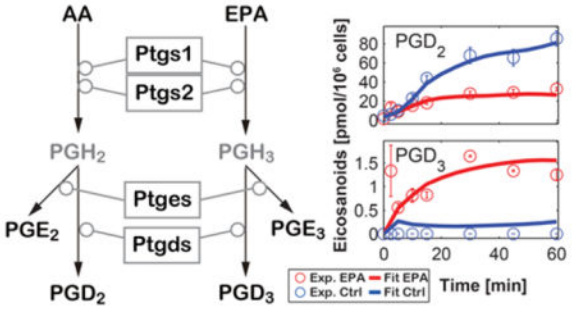

Introduction

We previously developed a novel approach to analyze the flux of arachidonic acid and its downstream metabolites in the murine macrophage-like RAW cell line implicated in eicosanoid biosynthesis initiated by the activation of phospholipase A_2 [1]. We also extended this model to bone marrow derived primary macrophages (BMDM) primed with the lipopolysaccharide (LPS) analogue KDO_2 -Lipid A followed by activation with a purinergic P2X7 receptor agonist ATP [2]. We have now analysed the effects of the ω3 polyunsaturated fatty acids (PUFAs) eicosapentaenoic acid (EPA; 5Z,8Z,11Z,14Z,17Z-eicosapentaenoic acid) and docosahexaenoic acid (DHA; 4Z,7Z,10Z,13Z,16Z,19Z-docosahexaenoic acid) on normal eicosanoid metabolism in murine macrophage cells [3].

Fatty acids (FAs) are considered as simple lipids and are comprised of a carbon chain and a terminal carboxylic acid. Saturated FAs, such as palmitic and stearic acids, have no double bonds and are *de novo* synthesized by chain elongation of an acetyl-CoA primer with malonyl-CoA. Stearic acid is further metabolized to longer-chain saturated FAs and also unsaturated FA like oleic acids. Due to the absence of desaturases, in *Homo sapiens,* for introducing a double bond into FAs distal to the Δ9 position, dietary supplementation of essential FAs (EFAs) is required. EFAs, including α-linolenic acid (9Z,12Z,15Z-octadecatrienoic acid) and linoleic acid (9Z,12Z-octadecadienoic acid), are elongated and desaturated in our body resulting in ω3 and ω6 polyunsaturated fatty acids (PUFAs), respectively. Arachidonic acid (AA; 5Z,8Z,11Z,14Z-eicosatetraenoic acid), a representative ω6 PUFA, is a precursor of prostaglandins (PGs), leukotrienes (LTs) and other oxygenated metabolites that play important roles in inflammation, cell-cell communication, and several pathophysiological conditions [4–6]. These lipid mediators, generically called eicosanoids, are produced on demand through the sequential actions of spatially and temporally regulated eicosanoid-synthesizing enzymes. The cyclooxygenases (COXs; COX-1 and -2), which are targets of non-steroidal anti-inflammatory drugs (NSAIDs) like aspirin, metabolize AA to

produce an unstable endoperoxide intermediate, PGH_2, and to produce two mono-hydroxylated side products, 11-hydroxy eicosatetraenoic acid (11-HETE) and 15-hydroxy eicosatetraenoic acid (15-HETE) simultaneously [7, 8]. Specific terminal enzymes metabolize PGH_2 to 2-series PGs such as PGD_2, PGE_2, $PGF_{2\alpha}$, PGI_2 and thromboxane A_2 (TXA_2) [7]. AA is also metabolized by 5-lipoxygenase (5-LOX) to 5-hydroxyeicosatetraenoic acid (5-HETE) and an unstable intermediate LTA_4, which is further metabolized to LTB_4 and LTC_4 [9–11].

The ω3 PUFAs, such as eicosapentaenoic acid (EPA; 5Z,8Z,11Z,14Z,17Z-eicosapentaenoic acid) and docosahexaenoic acid (DHA; 4Z,7Z,10Z,13Z,16Z,19Z-docosahexaenoic acid), are now widely used as a supplement for health benefits. Epidemiologic analyses demonstrate a lower prevalence of coronary heart disease in Greenland Eskimos (Inuits) [12], which is thought to be due to their diet like seal and whale that contain abundant ω3 PUFAs [13]. These epidemiological studies have been supported by several clinical trials suggesting that supplementation of ω3 PUFAs reduces the risk of cardiovascular events [12]. A possible mechanism of ω3 PUFA-mediated cardioprotection is a reduction in 2-series PG by competitive metabolism between AA and ω3 PUFAs, because EPA is metabolized to less potent 3-series PGs (like PGE_3 and PGD_3) by COX and terminal enzymes [14]. Indeed, long-term therapy with low-dose aspirin has been employed for the prevention of cardiovascular events [15], suggesting that suppression of 2-series PG production seems to be beneficial for reducing cardiovascular risks, though enhanced conversion to lipoxins may also contribute [16]. Another possible mechanism has been proposed that ω3 PUFAs are metabolized to anti -inflammatory/pro-resolving lipid mediators such as D-series and E-series resolvins, protectins, and maresins [17]. Although detailed mechanisms are not yet fully established, it is widely assumed that ω3 PUFA-containing diets are helpful in preventing cardiovascular and other diseases [12, 18].

A systems biology approach offers a powerful strategy to reveal novel mechanisms in cellular and molecular machinery. Indeed, we previously found important molecular interactions between lipid metabolic enzymes by developing a computational model [1, 2, 19]. In the present study, we developed a computational model for understanding the competitive metabolism of ω3 and ω6 PUFAs in macrophages that are one of the major inflammatory cells that produce eicosanoids and play pivotal roles in cardiovascular pathologies including atherosclerosis. Based on our original experimental data [3], kinetic parameters were estimated by a two-step matrix-based approach employing a constrained least-squares method followed by nonlinear optimization. The computational model was able to simulate another experimental conditions, using AA and DHA instead of EPA, indicating that the model is valid and useful for simulating the competitive metabolism between ω3 and ω6 PUFAs.

Methods

Development of kinetic models

The reaction rates were described by linear kinetics with the assumption that for enzymatic reactions, the substrate concentrations are much lower than the corresponding Michaelis constant, K_M. A quasi-steady state approximation, in which the enzyme-substrate complex production rate was assumed to be equal to that of dissociation rate, was used to describe the

competitive metabolism. If an enzyme E competitively catalyses different substrates S_1,…, S_j,…, S_N, and produces their products P_1,…, P_j,…, P_N, respectively, the total amount of enzyme E_{Total} is described as follows:

$$[E_{Total}]=[E_{Free}]+\sum_{j=1}^{N}[E{:}S_j] \quad (j=1,\ldots,N),$$

where [E:S_j] is a complex of enzyme E and substrate S_j. Therefore, the reaction rate of P_n formation from S_n by enzyme E is described as follows:

$$r_{p_n}=\frac{k_n[E_{total}][S_n]}{1+\sum_{j=1}^{N}K_j[S_j]} \quad (n=1,\ldots,N),$$

where K_n is a lumped rate constants related to the substrate S_n, and K'_j is the association constant between the enzyme E and the substrate S_j. For example, in the present study, the PGH_2 (P_n) production rate from AA (S_n) via COX (E) in the presence of EPA (S_j) is described as follows:

$$r_{PGH_2}=\frac{k_1[COX][AA]}{1+K_{COX:AA}[AA]+K_{COX:EPA}[EPA]+C_1}$$

where C_1 represents all other inhibitory mechanisms of COX. The ordinary differential equations (ODEs) were generated based on the rate of change of metabolites (mass-balance) using the reaction rates. All of the equations used in the simulation are listed in Appendix A.

Estimation of the kinetic rate parameters and uncertainty analysis

As previously reported [1, 2, 19], all the ODEs without the inhibitory kinetic parameters used in this study were rearranged in a matrix format, i.e., **Y** = **X** × **K**, where **Y** and **K** are matrices for metabolite concentrations and kinetic parameters, respectively. The quantitative data of **X** and **Y** was obtained from our original experimental results [3]. First, to estimate the matrix **K**, a least squares approach (Matlab® function lsqlin) was used constraining all the parameters to be positive. Then, initial guesses for the inhibitory parameters were added to the list of estimated parameters values from previous step. All the parameters values were further optimized by using generalized constrained nonlinear optimization (Matlab® function fmincon) where the objective function was to minimize the fit-error between the experimental and predicted metabolite concentrations.

$$\min_{K,X_0}\left(\sum_{i=1}^{nsp}\left(\sum_{j=1}^{nt}(y_{i,j,exp}-y_{i,j,pred}(K,X_0))^2\right)\right)$$

K: parameters (rate constants)

X_0: Initial conditions (metabolite concentrations)

where nt is the number of time-points and nsp is the number of metabolites. Numerical integration was used (e.g. Matlab® function ode23) to simulate the system to circumvent discretization error. The initial conditions were also optimized in a narrow range around the experimental values. The point-wise error was scaled by the square root of the length of the time interval for the purpose of resolving relatively poor fits by irregular time intervals. In the parameter estimation process, we optimized the profile for PGH_2 and PGH_3 formation with the constraint that its maximum concentration remains less than ~200 and ~10 pmol/million cells, respectively, based on the total amount of lipids produced, because we could not measure the level of PGH_2 and PGH_3.

The goodness of the fits was accessed by comparing the variance for the fitted data to the variance in the experimental (replicate) data (Treatment and Control data combined) using F-test as follows:

$$F=\frac{SSE_{fit}/(2\times nt\times nsp)}{SSE_{\exp}/(2\times nt\times nsp\times(nr-1))}$$
$$=\frac{\sum_{k=1}^{nsp}\left(\sum_{j=1}^{nt}(Y_j^{Trt}-\overline{X}_j^{Trt})^2+\sum_{j=1}^{nt}(Y_j^{Ctrl}-\overline{X}_j^{Ctrl})^2\right)/(2\times nt\times nsp)}{\sum_{k=1}^{nsp}\left(\sum_{j=1}^{nt}\sum_{i=1}^{nr}(X_{ij}^{Trt}-\overline{X}_j^{Trt})^2+\sum_{j=1}^{nt}\sum_{i=1}^{nr}(X_{ij}^{Ctrl}-\overline{X}_j^{Ctrl})^2\right)/(2\times nt\times nsp\times(nr-1))},$$

where X_j, $\bar{X}_j$ and Y_j denote the experimental data, mean experimental data and simulated (fitted) data at time point j, respectively, nr is the number of replicates (nr = 3, indexed as i), and Trt and Ctrl are treatment and control groups, respectively. F smaller than $F_{th} = F_{0.95}(128, 256) = 1.28$ indicates statistically equal variance in simulated (fitted) and experimental data.

The uncertainty analysis was performed on the parameters to evaluate the variation of estimated rate constants as previously described [2]. Briefly, the nsp × nt normally distributed data matrix was generated using the mean-value of the experimental lipid data and the corresponding standard-error of means (SEMs) at each time point. The parameter estimation was performed using this data set, and repeated k times (k = 10 in our simulation). The SEM for each parameter across the k sets was computed.

Results and Discussion

Development of the kinetic model for the COX pathway

The chemical structures of AA, EPA and DHA are shown in Fig 1A. RAW264.7 macrophages were cultured in the absence or presence of supplemental 25 μM AA, EPA and DHA for 24 hrs prior to ATP stimulation, and then culture supernatants were collected at the indicated time points (Fig. 1B). The quantitative data was reported previously [3] and was used in the present study. In our previous study, ATP-stimulated RAW264.7 macrophages produced high amount of eicosanoids within an hour, which was not affected by the inhibitors of transcription and translation of cellular proteins, suggesting that the levels of eicosanoid-synthesizing enzymes were unchanged and are negligible [20]. Therefore, we

developed a computational model without distinguishing COX isozymes as previously reported [2]. Figure 1C illustrates a COX-mediated lipid metabolic network [1]. The competitive metabolism between AA and EPA were modelled according to the quasi-steady state approximation as described in Methods. The model was described by linear kinetics based on the law-of-mass action and composed of 10 ODEs with 29 kinetic parameters. All ODEs are given in the Appendix A.

Next, we estimated the effective rate constants using EPA-supplemented and non-supplemented (control) data using the matrix-based two-step approach described in Methods. With the optimized parameters, a good fit (F score = 0.30 < F_{th}) to the experimental lipid profiles was achieved (Figure 1D). An uncertainty analysis was performed on the optimized parameters to assess the effect of a variation in the experimental data. The SEM for each parameter across the 10 sets of analysis was computed and is given in Table 1. Most of the parameters showed less than 25% variation. In the case of some of the parameters associated with degradation reactions or appearing in the denominator of the reaction-rate expression, high relative-fluctuations were observed, possibly as a mathematical artifact.

Parametric sensitivity, time scale analysis and validation of the model

Parametric sensitivity analysis was performed to test the robustness of the model. Each optimized parameter was individually changed in a range between two-fold up and down from the optimized parameter and responses were predicted. To perform the sensitivity analysis on AA, EPA and DHA, the whole profiles of AA, EPA and DHA were increased or decreased. The slope of the sensitivity curve for each parameter and each metabolite was calculated and displayed as a heat map (Figure 2A). With most of the parameters, small to moderate sensitivities were observed, and the sensitivities were consistent with the structure of the biochemical reaction network (Figure 1B). For example, changing the parameter of AA→PGH_2, k_{C1}, tended to increase AA metabolites and decrease PGE_3, whereas changing the parameter of EPA→PGH_3, k_{C15}, showed an increase of EPA metabolites and no or a slight increase of AA metabolites. The EPA association constant, $K_{COX:EPA}$, also reflected the structure of the AA/EPA metabolic network, which showed the opposite effects of AA and EPA on the 2-series and 3-series eicosanoid production. However, changing the AA association constant, $K_{COX:AA}$, did not produce significant effects on any of the eicosanoids. These results suggest that our model of eicosanoid metabolism is robust with respect to parametric perturbations.

To test the validity of the model, one of the intermediary metabolites, PGD_2, was excluded from the objective function and we simulated the profiles. The values of the estimated parameters in this leave-one-metabolite-out method were similar to those of corresponding optimized parameters (Figure 2C), and the simulated time-courses were in good agreement with the experimental time-courses qualitatively and quantitatively (Figure 2B).

To understand the kinetic features of the cellular responses, a timescale analysis was performed by computing eigenvalues and eigenvectors of the Jacobian matrix of the ODEs at steady state conditions. The timescale was divided into two ranges (i.e., fast, and slow) depending upon the eigenvalues and metabolites significantly contributing to the

corresponding eigenvectors. Time scales of most of the metabolites were similar to our previous analysis of the eicosanoid pathway [2]. Most of the AA and EPA metabolites (PGE_2, PGD_2, PGJ_2, 15d-PGJ_2, 11-HETE, PGE_3 and PGD_3) were distributed mainly in the slow timescale. However, PGH_2 and PGH_3 showed a fast timescale because of their low concentrations and unstable nature.

To check the reliability of optimized parameters, the fluxes for PGD_2 and PGE_2 were compared with the literature values. Urade *et al.* reported that the PGD_2 flux in macrophages is less than 30 pmol/min/million cells [21]. The activity of purified mouse mPGES-1 has been reported to be about 100 nmol/min/mg of purified enzyme, which is equivalent to 0.1 pmol/min/million cells [22]. We converted the activity of purified mouse mPGES-1 using the experimentally obtained values of 0.25 mg of total protein, and 1 ng of mPGES-1 protein are present in 10^6 cells [1, 23]. In our model, the calculated PGD_2 and PGE_2 fluxes at steady state were 1.2 and 0.23 pmol/min/million cells, respectively. Considering the differences in the experimental conditions, cell types, inaccuracies in some of the modeling approximations, etc., such differences in the parameter values between the present and previous studies are acceptable.

Prediction of eicosanoid profile in AA-supplemented and DHA supplemented macrophages

We further validated our computational model by predicting the eicosanoid profiles in AA-supplemented ATP-stimulated RAW264.7 macrophages. The optimized parameters did not predict the profiles well. Therefore, the parameters were re-optimized by allowing 25% variability in the optimized parameter values. The range of 25% variability was chosen based on the uncertainty analysis of the optimized parameters (Table 1). The simulation results with the re-optimized parameters showed a good fit between the predicted time-course and the experimental data (Figure 3A), suggesting that the optimized parameters are useful for predicting other eicosanoid profiles in RAW264.7 cells.

DHA, as well as EPA, effectively inhibit eicosanoid production through COX inhibition [24]. Therefore, the eicosanoid profiles in DHA-supplemented ATP-stimulated RAW264.7 macrophages were also predicted after re-optimizing the parameters again within 25% of the values reported in Table 1. To account for the DHA inhibition, the association constant between COX and DHA, $K_{COX:DHA}$, was added in the ODEs. The optimized value of $K_{COX:DHA}$ was 0.1629 1/pmol/10^6 cells). The simulation results showed a good fit between the predicted time-course and the experimental data (Figure 3B). Collectively, optimized parameters are reliable in predicting eicosanoid profiles, and the mathematical model reflects the eicosanoid metabolic network in macrophages.

Simulation of COX activities during AA/EPA supplementation

Wada *et al.* reported that COX-1 could not utilize EPA as a substrate, but that EPA inhibited COX-1 activity [14]. Further, EPA was metabolized by COX-2 to PGH_3 and barely inhibited COX-2 activity [14]. Within the 60 minute time-frame of our study, we could not detect significant expression changes of COXs in ATP stimulated macrophages [3], and thus we did not distinguish between COX-1 and COX-2 in the model. Previous studies indicated that the

basal protein expression level of COX-2 is about 5% as compared to COX-1 expression [2]. The less than 5% concentration of EPA metabolites compared to the total concentration of all metabolites in the experimental data (Figure 2) was consistent with the basal protein expression level of COX-1 and COX-2. The same effect was also seen in flux values. In our model, COX metabolized AA and EPA at the rate of 4 and 0.2 pmol/min/million cells, respectively. To further understand the inhibitory effect of EPA *in vivo*, we simulated how EPA supplementation would affect the COX activities (Figure 4). EPA supplementation inhibited COX activities in a dose dependent manner (Figure 4A), whereas its metabolism was less affected by AA supplementation (Figure 4B). These distinct responses were due to the difference in the values of KCOX:AA and KCOX:EPA (~ 25* KCOX:AA) which reflects AA and EPA affinity/binding to COX, respectively. Taken together, our model captured features of both COX-1 and COX-2.

Our modeling approach has helped validate the mechanism of ω3 PUFA -mediated reduction in 2-series PG by competitive metabolism between AA and ω3 PUFAs by COX and terminal enzymes. This model can be used in systems pharmacokinetics and pharmacodynamics studies to calculate inhibition efficiency of drugs and to design dose schedule for inflammation and immune system related diseases. Previously, we have carried out an in-depth comparison of transcriptomic and lipidomic response of RAW264. 7 and thioglycolate-elicited macrophages to KLA [25]. Overall, RAW 264.7 cells serve as a good model for studying inflammation and immunity associated with primary macrophages. However, their responses to different ligands can differ in term of time scale and kinetics. For example, ATP stimulated RAW264.7 cells produce eicosanoids in a time-scale of 1 hour [20], whereas ATP-stimulated bone marrow-derived macrophages produce prolonged production of eicosanoids lasting 20 hours [2, 26].

Conclusion

We have developed a quantitative model of the competitive metabolism of AA and EPA via the COX pathway by integrating known mechanistic knowledge and novel high-throughput data in RAW 264.7 macrophages. The robustness of the model is validated through parametric sensitivity and uncertainty analysis. Additionally, we have successfully predicted the eicosanoid profiles in independent datasets utilizing AA and DHA instead of EPA. The computational model developed has enhanced our understanding of the biological characteristics of eicosanoid metabolic networks. We showed that the higher affinity of EPA binding to COX compared to AA was able to inhibit AA metabolism effectively. Thus, our computational model helps to elucidate the competition between ω3 and ω6 metabolism in cells as an *ex vivo* model of inflammation.

Acknowledgments

It is an honor to contribute this article to Professor McCammon’s Festschrift. His contributions to Chemical Physics, Physical Chemistry and Biological Physics are legendary. This work was supported by NIH grants RO1 GM20,501-40 (EAD), the LIPID MAPS “Glue” Grant U54 GM069338 (EAD, SS), U01 DK097430 (SS) and an NSF grant STC-0939370 (SS).

References

1. Gupta S, Maurya MR, Stephens DL, Dennis EA, Subramaniam S. An integrated model of eicosanoid metabolism and signaling based on lipidomics flux analysis. Biophysical journal. 2009; 96(11):4542–4551. [PubMed: 19486676]
2. Kihara Y, Gupta S, Maurya MR, Armando A, Shah I, Quehenberger O, Glass CK, Dennis EA, Subramaniam S. Modeling of eicosanoid fluxes reveals functional coupling between cyclooxygenases and terminal synthases. Biophysical journal. 2014; 106(4):966–975. [PubMed: 24559999]
3. Norris PC, Dennis EA. Omega-3 fatty acids cause dramatic changes in TLR4 and purinergic eicosanoid signaling. Proceedings of the National Academy of Sciences of the United States of America. 2012; 109(22):8517–8522. [PubMed: 22586114]
4. Dennis EA, Norris PC. Eicosanoid storm in infection and inflammation. Nature reviews Immunology. 2015; 15(8):511–523.
5. Buczynski MW, Dumlao DS, Dennis EA. Thematic Review Series: Proteomics. An integrated omics analysis of eicosanoid biology. Journal of lipid research. 2009; 50(6):1015–1038. [PubMed: 19244215]
6. Quehenberger O, Dennis EA. The human plasma lipidome. The New England journal of medicine. 2011; 365(19):1812–1823. [PubMed: 22070478]
7. Smith WL, DeWitt DL, Garavito RM. Cyclooxygenases: structural, cellular, and molecular biology. Annual review of biochemistry. 2000; 69:145–182.
8. Hemler ME, Crawford CG, Lands WE. Lipoxygenation activity of purified prostaglandin-forming cyclooxygenase. Biochemistry. 1978; 17(9):1772–1779. [PubMed: 26389]
9. Radmark O, Werz O, Steinhilber D, Samuelsson B. 5-Lipoxygenase, a key enzyme for leukotriene biosynthesis in health and disease. Biochimica et biophysica acta. 2015; 1851(4):331–339. [PubMed: 25152163]
10. Kanaoka Y, Boyce JA. Cysteinyl leukotrienes and their receptors; emerging concepts. Allergy, asthma & immunology research. 2014; 6(4):288–295.
11. Yokomizo T. Leukotriene B4 receptors: novel roles in immunological regulations. Advances in enzyme regulation. 2011; 51(1):59–64. [PubMed: 21035496]
12. De Caterina R. n-3 fatty acids in cardiovascular disease. The New England journal of medicine. 2011; 364(25):2439–2450. [PubMed: 21696310]
13. Bang HO, Dyerberg J, Sinclair HM. The composition of the Eskimo food in north western Greenland. The American journal of clinical nutrition. 1980; 33(12):2657–2661. [PubMed: 7435433]
14. Wada M, DeLong CJ, Hong YH, Rieke CJ, Song I, Sidhu RS, Yuan C, Warnock M, Schmaier AH, Yokoyama C, et al. Enzymes and receptors of prostaglandin pathways with arachidonic acid-derived versus eicosapentaenoic acid-derived substrates and products. The Journal of biological chemistry. 2007; 282(31):22254–22266. [PubMed: 17519235]
15. Patrono C, Garcia Rodriguez LA, Landolfi R, Baigent C. Low-dose aspirin for the prevention of atherothrombosis. The New England journal of medicine. 2005; 353(22):2373–2383. [PubMed: 16319386]
16. Norris PC, Gosselin D, Reichart D, Glass CK, Dennis EA. Phospholipase A2 regulates eicosanoid class switching during inflammasome activation. Proceedings of the National Academy of Sciences of the United States of America. 2014; 111(35):12746–12751. [PubMed: 25139986]
17. Serhan CN. Pro-resolving lipid mediators are leads for resolution physiology. Nature. 2014; 510(7503):92–101. [PubMed: 24899309]
18. Khawaja OA, Gaziano JM, Djousse L. N-3 fatty acids for prevention of cardiovascular disease. Current atherosclerosis reports. 2014; 16(11):450. [PubMed: 25214423]
19. Gupta S, Maurya MR, Merrill AH Jr, Glass CK, Subramaniam S. Integration of lipidomics and transcriptomics data towards a systems biology model of sphingolipid metabolism. BMC systems biology. 2011; 5:26. [PubMed: 21303545]
20. Buczynski MW, Stephens DL, Bowers-Gentry RC, Grkovich A, Deems RA, Dennis EA. TLR-4 and sustained calcium agonists synergistically produce eicosanoids independent of protein

synthesis in RAW264.7 cells. The Journal of biological chemistry. 2007; 282(31):22834–22847. [PubMed: 17535806]

21. Urade Y, Ujihara M, Horiguchi Y, Igarashi M, Nagata A, Ikai K, Hayaishi O. Mast cells contain spleen-type prostaglandin D synthetase. J Biol Chem. 1990; 265(1):371–375. [PubMed: 2403560]
22. Lazarus M, Kubata BK, Eguchi N, Fujitani Y, Urade Y, Hayaishi O. Biochemical characterization of mouse microsomal prostaglandin E synthase-1 and its colocalization with cyclooxygenase-2 in peritoneal macrophages. Arch Biochem Biophys. 2002; 397(2):336–341. [PubMed: 11795891]
23. Boulet L, Ouellet M, Bateman KP, Ethier D, Percival MD, Riendeau D, Mancini JA, Methot N. Deletion of microsomal prostaglandin E2 (PGE2) synthase-1 reduces inducible and basal PGE2 production and alters the gastric prostanoid profile. J Biol Chem. 2004; 279(22):23229–23237. [PubMed: 15016822]
24. Yuan C, Sidhu RS, Kuklev DV, Kado Y, Wada M, Song I, Smith WL. Cyclooxygenase Allosterism, Fatty Acid-mediated Cross-talk between Monomers of Cyclooxygenase Homodimers. The Journal of biological chemistry. 2009; 284(15):10046–10055. [PubMed: 19218248]
25. Maurya MR, Gupta S, Li X, Fahy E, Dinasarapu AR, Sud M, Brown HA, Glass CK, Murphy RC, Russell DW, et al. Analysis of inflammatory and lipid metabolic networks across RAW264.7 and thioglycolate-elicited macrophages. Journal of lipid research. 2013; 54(9):2525–2542. [PubMed: 23776196]
26. Dinasarapu AR, Gupta S, Ram Maurya M, Fahy E, Min J, Sud M, Gersten MJ, Glass CK, Subramaniam S. A combined omics study on activated macrophages--enhanced role of STATs in apoptosis, immunity and lipid metabolism. Bioinformatics. 2013; 29(21):2735–2743. [PubMed: 23981351]

Appendix A

$$\frac{\mathrm{d}[\mathrm{PGH_2}]}{\mathrm{dt}}=\frac{k_{C1}[\mathrm{AA}]}{1+K_{\mathrm{COX:AA}}[\mathrm{AA}]+K_{\mathrm{COX:EPA}}[\mathrm{EPA}]+C_1}-(k_{\mathrm{C2}}+\frac{k_{C3}}{1+K_{\mathrm{PGES:PGH2}}[\mathrm{PGH_2}]+K_{\mathrm{PGES:PGH3}}[\mathrm{PGH_3}]+C_2}+\frac{k_{C5}}{1+K_{\mathrm{PGDS:PGH2}}[\mathrm{PGH_2}]+K_{\mathrm{PGDS:PGH3}}[\mathrm{PGH_3}]+C_3}$$

$$\frac{\mathrm{d}[\mathrm{PGE_2}]}{\mathrm{dt}}=\frac{k_{C3}[\mathrm{PGH_2}]}{1+K_{\mathrm{PGES:PGH2}}[\mathrm{PGH_2}]+K_{\mathrm{PGES:PGH3}}[\mathrm{PGH_3}]+C_2}-k_{C4}[\mathrm{PGE_2}]$$

$$\frac{\mathrm{d}[\mathrm{PGD_2}]}{\mathrm{dt}}=\frac{k_{C5}[PGH_2]}{1+K_{\mathrm{PGDS:PGH2}}[\mathrm{PGH_2}]+K_{\mathrm{PGDS:PGH3}}[\mathrm{PGH_3}]+C_3}-(k_{C6}+k_{C7}+k_{C9}+k_{C11})[\mathrm{PGD_2}]$$

$$\frac{\mathrm{d}[\mathrm{DHKPGD_2}]}{\mathrm{dt}}=k_{C7}[\mathrm{PGD_2}]-k_{C8}[\mathrm{DHKPGD_2}]$$

$$\frac{\mathrm{d}[\mathrm{15dPGD_2}]}{\mathrm{dt}}=k_{C9}[\mathrm{PGD_2}]-k_{C10}[\mathrm{15dPGD_2}]$$

$$\frac{\mathrm{d}[\mathrm{PGJ_2}]}{\mathrm{dt}}=k_{C11}[\mathrm{PGD_2}]-k_{C12}[\mathrm{PGJ_2}]$$

$$\frac{\mathrm{d}[11-\mathrm{HETE}]}{\mathrm{dt}}=\frac{k_{C13}[\mathrm{AA}]}{1+K_{\mathrm{COX:AA}}[\mathrm{AA}]+K_{\mathrm{COX:EPA}}[\mathrm{EPA}]+C_1}-k_{C14}[11-\mathrm{HETE}]$$

$$\frac{\mathrm{d}[\mathrm{PGH_3}]}{\mathrm{dt}}=\frac{k_{C15}[\mathrm{EPA}]}{1+K_{\mathrm{COX:AA}}[\mathrm{AA}]+K_{\mathrm{COX:EPA}}[\mathrm{EPA}]+C_1}-(k_{\mathrm{C16}}+\frac{k_{C17}}{1+K_{\mathrm{PGES:PGH2}}[\mathrm{PGH_2}]+K_{\mathrm{PGES:PGH3}}[\mathrm{PGH_3}]+C_2}+\frac{k_{C18}}{1+K_{\mathrm{PGDS:PGH2}}[\mathrm{PGH_2}]+K_{\mathrm{PGDS:PGH3}}[\mathrm{PGH_3}]+C_3}$$

$$\frac{\mathrm{d}[\mathrm{PGE_3}]}{\mathrm{dt}}=\frac{k_{C17}[\mathrm{PGH_3}]}{1+K_{\mathrm{PGES:PGH2}}[\mathrm{PGH_2}]+K_{\mathrm{PGES:PGH3}}[\mathrm{PGH_3}]+C_2}-k_{C19}[\mathrm{PGE_3}]$$

$$\frac{\mathrm{d}[\mathrm{PGD_3}]}{\mathrm{dt}}=\frac{k_{C18}[\mathrm{PGH_3}]}{1+K_{\mathrm{PGDS:PGH2}}[\mathrm{PGH_2}]+K_{\mathrm{PGDS:PGH3}}[\mathrm{PGH_3}]+C_3}-k_{C20}[\mathrm{PGD_3}]$$

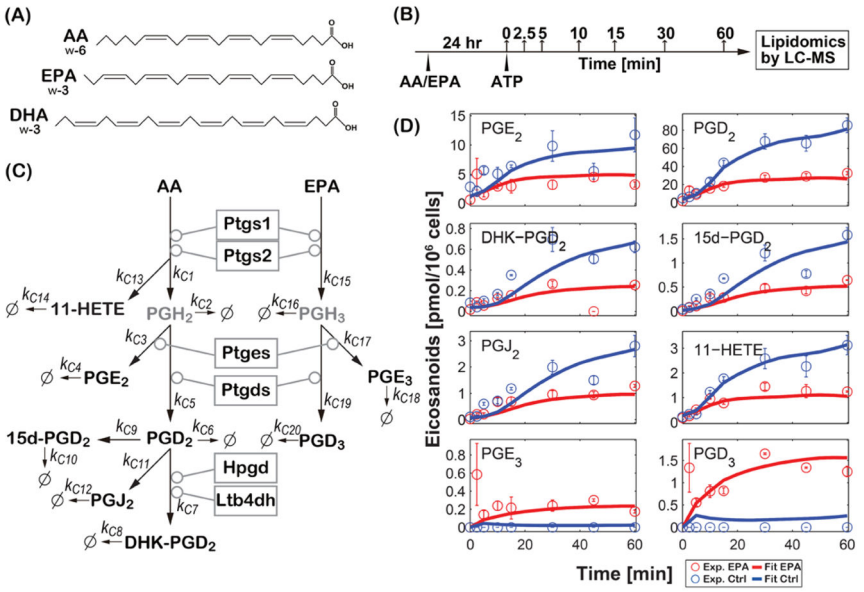

Figure 1. Computational simulation of the COX-dependent eicosanoid profiles in EPA-supplemented ATP-stimulated RAW264.7 cells

(A) The chemical structures of AA, EPA and DHA. (B) Experimental conditions. AA and EPA were supplemented in RAW264.7 cell culture media for 24 hr before stimulation. Then, cells were stimulated with ATP and the culture media were collected at the indicated time points to measure the eicosanoid levels by liquid chromatography-tandem mass spectrometry (LC-MS). (C) Simplified AA and EPA metabolic pathways via the COX pathway. The measured and non-measured metabolites are given in black and gray letters, respectively. Arrows indicate the enzymatic and non-enzymatic reactions and the Ø symbol represents additional metabolic pathways including degradation. (D) The experimental data (Exp) for EPA and non-supplement represent means ± SEM. The simulation results (Fit) are shown as red and blue curves for EPA supplemented and non-supplemented data, respectively.

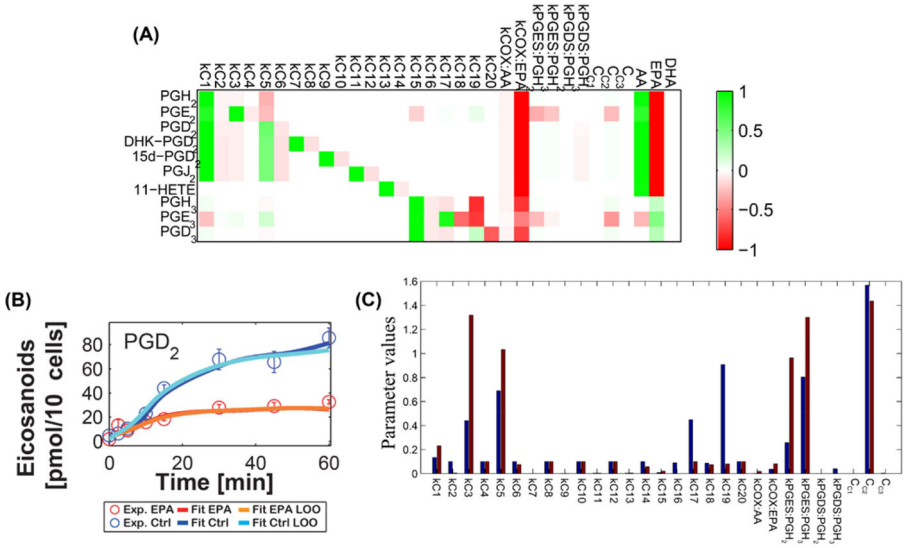

Figure 2. Parametric sensitivity analysis and leave-one-metabolite-out analysis

(A) Slope of the sensitivity curves are shown as heat maps. Sensitivity of KCOX:EPA and EPA was found in the range of −4 – 0.5. (B) The simulation results of leave-one-metabolite (PGD_2)-out are shown as orange and light blue curves for EPA supplemented and non-supplemented data, respectively. The blue and red lines are simulation results obtained from Fig. 1D. (C) The estimated parameters by leave-one-metabolite (PGD_2)-out methods are compared with optimized parameters.

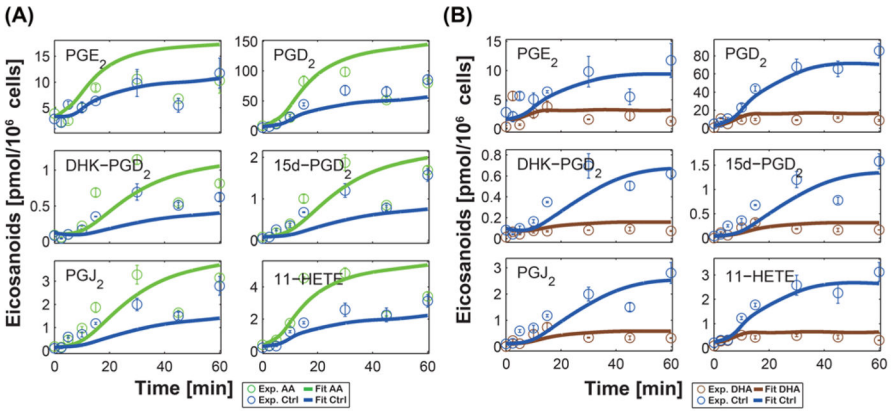

Figure 3. Computational prediction of COX-dependent eicosanoid profile in AA and DHA-supplemented ATP-stimulated RAW264.7

(A) The experimental data (Exp) for non-supplemented and AA-supplemented cases represent means ± SEM. The simulation results (Fit) are shown as green and blue curves for AA-supplemented and non-supplemented, respectively. (B) The experimental data (Exp) for non-supplemented and DHA-supplemented cases represent means ± SEM. The simulation results (Fit) are shown as brown and blue curves for DHA-supplemented and non-supplemented cases, respectively.

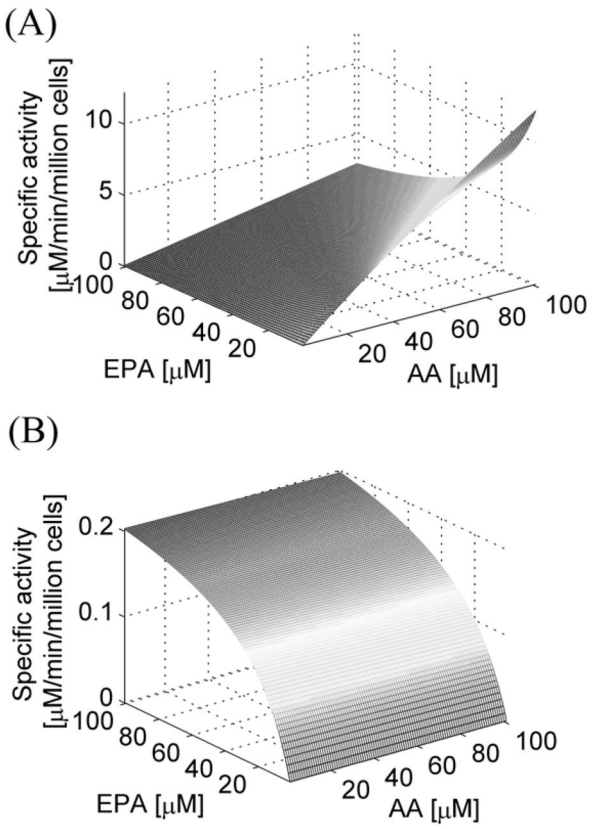

Figure 4. Computational simulation of COX activities

(A) The COX specific activities for AA were simulated with increasing concentrations of AA in the presence of EPA. (B) The COX specific activities for EPA were simulated with increasing concentrations of EPA in the presence of AA.

Table 1

Chemical reactions and estimated kinetic parameters in the COX pathway

Reaction	Name	Parameters Optimized value	SEM
AA → PGH2	kC1	0.1353	0.0361
PGH2 →	kC2	0.1	0.0142
PGH2 → PGE2	kC3	0.4399	0.2996
PGE2 →	kC4	0.1	0.0101
PGH2 → PGD2	kC5	0.6906	0.1823
PGD2 →	kC6	0.1	0.0118
PGD2 → DHKPGD2	kC7	0.0009	0.0001
DHKPGD2 →	kC8	0.1	0.0001
PGD2 → 15dPGD2	kC9	0.0019	0.0002
15dPGD2 →	kC10	0.1	0.0000
PGD2 → PGJ2	kC11	0.0036	0.0002
PGJ2 →	kC12	0.1	0.0014
AA → 11-HETE	kC13	0.0039	0.0020
11-HETE →	kC14	0.1	0.0083
EPA → PGH3	kC15	0.0094	0.0161
PGH3 →	kC16	0.0904	0.0128
PGH3 → PGE3	kC17	0.4489	0.0638
PGE3 →	kC18	0.0873	0.0116
PGH3 → PGD3	kC19	0.9075	0.2395
PGD3 →	kC20	0.1	0.0057
	KCOX:AA	0.0014	0.0145
	KCOX:EPA	0.0366	0.0720
	KPGES:PGH2	0.2569	0.1715
	KPGES:PGH3	0.8046	0.4272
	KPGDS:PGH2	0	0.0483
	KPGDS:PGH3	0.0411	0.1238
	CC1	0	0.0064
	CC2	1.5659	0.7107
	CC3	0.004	0.0633

The unit of the parameters in first-order reactions is 1/min. Association constants such as KCOX:AA have units of 1/concentration.